LOCATION OF CARBONATE IONS IN STRUCTURE OF BIOLOGICAL APATITE

Michael E. Fleet and Xi Liu
University of Western Ontario
Department of Earth Sciences
London, Ontario N6A 5B7

ABSTRACT

Substitution of the carbonate ion into the channel (A) and phosphate group (B) positions of hydroxyapatite (CHAP), fluorapatite (CFAP) and chlorapatite (CCLAP) has been investigated by Fourier transform infrared (FTIR) spectroscopy and single-crystal X-ray structure, using crystals synthesized at high pressure and temperature (0.5-1.0 GPa, 1000-1350°C). Based on similarity of chemical compositions and FTIR spectra, biological apatites appear to have the crystal structure of synthetic Na-bearing type A-B CHAP. Type A carbonate is oriented in the apatite channel with two oxygen atoms close to the *c*-axis and the third projecting close to the channel wall, whereas type B is located near the sloping faces of the substituted phosphate group. The Na-bearing carbonate apatite crystals have compositions corresponding approximately to the composition series $Ca_{10-y}Na_y[(PO_4)_{6-y}(CO_3)_y][(OH/Cl)_{2-2x}(CO_3)_x]$, with $x \approx y$ up to 1.0 for CHAP and 0.4 for CCLAP, and $Ca_{10-1.5y}Na_{y\ 0.5y}[(PO_4)_{6-2y}(CO_3)_{2y}][F_{2-2x}(CO_3)_x]$, with $x \approx y \approx 0.1$ for CFAP, for equivalent conditions of synthesis. The Na^+ cation and A and B carbonate ion defects are locally coupled in the structures of all three composition series to minimize the effects of charge compensation and spatial accommodation.

INTRODUCTION

The apatite-type structure is adopted by numerous inorganic compounds of general formula $M1_2M2_3(BO_4)_3X$, where M1 and M2 are large cations, B metalloids and X halides or oxy-anions (1,2). The calcium phosphate apatites [$Ca1_4Ca2_6(PO_4)_6X_2$] have an important geochemical role because they sequester phosphorus, rare earth elements, actinides, and volatile elements in the Earth's crust and mantle. These apatite-group minerals are dominantly solid solutions of hydroxyapatite [HAP; ideally $Ca_{10}(PO_4)_6(OH)_2$; $Z = 1$], fluorapatite [FAP; $Ca_{10}(PO_4)_6F_2$] and chlorapatite [CLAP; $Ca_{10}(PO_4)_6Cl_2$]. The natural phases all have the hexagonal space group $P6_3/m$, although pure, end-member HAP and CLAP crystallize in the monoclinic space group $P2_1/b$ (3). Carbonate-bearing HAP (presently abbreviated as CHAP) is by far the most important biomineral, accounting for up to about 65 % of cortical bone and 97 % of dental enamel, fluoride hosted by CHAP is the important anticaries component of dental enamel (4,5). CHAP and carbonated FAP (CFAP) are the dominant minerals in phosphorites (6), and FAP is a candidate phase for the containment of high-level nuclear waste. We note that, although the apatite species of bone is generally understood to be CHAP, structurally-bound hydroxyl is commonly not detected by spectroscopic studies (including infra-red, Raman, and nuclear magnetic resonance) on mineralized tissue extracted from bone (e.g. 7), but these null results are probably attributable to the procedures used for processing the mineralized tissues (8,9).

The hexagonal $P6_3/m$ structure of Ca apatites is well known. Apatite is an orthophosphate. Isolated PO_4 tetrahedra centered at z = 1/4,3/4 are linked by Ca1 in ninefold (6+3) coordination and Ca2 in an irregular sevenfold (6+1) coordination (Fig. 1a). A prominent feature of the structure is the large c-axis channel which accommodates

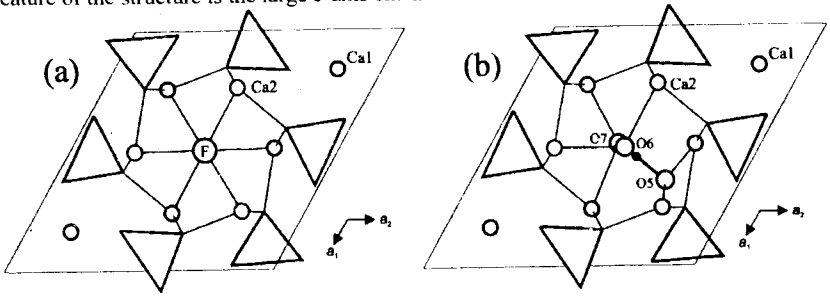

Figure 1. (a) Structure of fluorapatite; (b) location of type A carbonate in channel of CHAP: shaded phosphate polyhedra and Ca2 atoms are centered at z = 3/4.

the X anion component (F, OH and Cl). The apatite channel is defined by triclusters of Ca2 cations at z = 1/4,3/4. In fluorapatite (FAP), the F anion is located on the c-axis at z = 1/4,3/4 in the center of a tricluster of Ca2. OH in HAP and Cl in CLAP are displaced along the c-axis and have split atom positions with occupancy of 0.5: the hydroxyl oxygen is at $z = \pm(0.198,0.302)$ and the much larger Cl anion is displaced further at $z = \pm(0.432,0.068)$ (3). Thus, the coordination of the X anion is equilateral triangular in FAP but near octahedral in CLAP.

The structural role of carbonate in HAP and FAP has been investigated extensively by X-ray powder and single-crystal and neutron powder diffraction methods (e.g. 10-21,24). It has been established that the carbonate ion can be accommodated either in the c-axis structural channel or as a substituent for the phosphate group: the former carbonate is known as type A and the latter as type B. However, the structural details and estimation of the proportion of types A and B carbonate remain controversial. Structure analysis has been frustrated by several factors, including: (1) the limited substitution of carbonate (especially of type B carbonate), (2) small (nanoscale) crystal size of biological and inorganically precipitated apatite and of francolite from phosphorites, (3) poor crystallinity, and (4) weak and overlapped electron densities of carbonate atoms. We presently report on studies of the accommodation of carbonate in Na-bearing CHAP, CFAP and CCLAP using the X-ray single-crystal structure method and crystals grown from carbonate-rich melts at high pressure. The X-ray structure site occupancies are then used to interpret the characteristic carbonate bands in the infra-red spectra of these materials. We show that the CHAP crystal products, in particular, are appropriate analogues for the overall structural features of apatite biomaterials. The research on CHAP and CFAP has been reported in a number of recent papers (18-24), but this is the first review and synthesis of these studies; the CCLAP structures are work in progress).

EXPERIMENTAL PROCEDURES

High-pressure experiments were made using a Depths of the Earth Company Quickpress piston-cylinder device and a ¾ inch assembly. Synthesis conditions for Na-free CHAP are described elsewhere (18,22). Starting compositions for Na-bearing CHAP, CFAP and CCLAP were prepared from appropriate mixtures of analytical grade $CaHPO_4$, $Ca_2P_2O_7$, CaO, Na_2CO_3, $Ca(OH)_2$, $CaCO_3$, CaF_2, and $CaCl_2$. These salts were mixed in stoichiometric proportions corresponding to nominal type B carbonate apatite formulae {e.g. $Ca_8Na_2[(PO_4)_6(CO_3)_2]F_2$} with selected components (e.g. H_2O, CO_2, CaF_2, and Na_2CO_3) in excess. For each experiment, the starting mixture was encapsulated in a sealed platinum tube with a diameter of 5 mm and a height of 10 mm, which was separated from a graphite tube by an MgO sleeve. Run conditions are summarized in Table I. All experiments were quenched at pressure by switching off the furnace.

Table I. Synthesis of Na-bearing Carbonate Apatites

Composition Series[a]	Number of Experiments; X-ray Structures	*T* (°C)	*P* (GPa)	Time (hours)	Proportion of Na:A:B Carbonate	Maximum CO_2 (wt.%)
CHAP	4; 2	1200	1-0.5	8-16	1:1:1	8.2
CFAP	6; 4	1300-1150[b]	1	24-66	1:1:2	1.9
CCLAP	9; 3	1350-1000[b]	1	24-40	1:1:1-2	4.6

Note: [a] CHAP is carbonated hydroxyapatite; CFAP is carbonated fluorapatite; CCLAP is carbonated chlorapatite

[b] Melted at 1300-1350°C and annealed at lower temperature

Experimental products were characterized by optical microscopy, powder X-ray diffraction (Rigaku D/MAX-B system; Co *K*α X-radiation), electron probe micro-analysis (EPMA; JEOL JXA-8600), and Fourier transform infrared (FTIR) spectroscopy (Nicolet Nexus 670 FTIR spectrometer). Infrared spectra were obtained for hand-separated apatite crystals using KBr pellets (Fig. 2). Single-crystal X-ray diffraction measurements were made at room temperature and pressure with a Nonius Kappa CCD diffractometer and graphite-monochromatized Mo *K*α X-radiation (50 kV, 32 mA, $\lambda = 0.7107$ Å). Procedures for data reduction and structure analysis followed our previous studies (18,19,22). Summary results are given in Tables II and III, and a representative set of refined structure parameters, for CHAP (experiment LM005), in Table IV. Structural details and supporting arguments for Na-bearing CHAP and CFAP are reported in Refs. 21 and 24, respectively, and for CCLAP will be published elsewhere.

RESULTS AND DISCUSSION

The experimental products were carbonate apatite in the form of relatively large (up to 250 μm diameter) hexagonal prisms, which had evidently crystallized from the melt at the experimental temperature, and a fine-grained matrix of apatite and minor carbonates of quench origin. The FTIR spectra and X-ray structures revealed that the uptake of carbonate by Na-bearing apatite varied markedly from one composition series to another for similar conditions of

synthesis, being greatest for CHAP, with a maximum amount of 8.2 wt.% CO_2, least for CFAP at 1.9 wt.%, and intermediate for CCLAP at 3.4 wt.%. Several experiments on CFAP and CCLAP were subjected to a two-stage heating in an attempt to investigate the effect of temperature on the extent of carbonate

Table II. Details for Refinement of Na-bearing Structures

Apatite	Expt	a (Å)	c (Å)	D_x (g/cm^3)	R^a	R_w	S
CHAP[a]	LM005	9.3855(7)	6.9142(4)	3.12	0.023	0.014	0.60
	LM006	9.397(1)	6.889(1)	3.15	0.027	0.023	1.48
CFAP	LM130	9.3648(4)	6.8879(2)	3.176	0.019	0.019	1.11
	LM136	9.3679(3)	6.8885(3)	3.173	0.022	0.026	1.67
	LM142	9.3659(3)	6.8901(4)	3.124	0.023	0.021	1.14
CCLAP	LM169	9.5321(4)	6.8448(3)	3.055	0.027	0.025	1.33
	LM171	9.5121(4)	6.8603(4)	3.129	0.030	0.025	1.13
	LM173	9.5252(2)	6.8522(2)	2.969	0.033	0.026	1.93

Note: [a] R is residual index; R_w is weighted residual index; S is goodness-of-fit

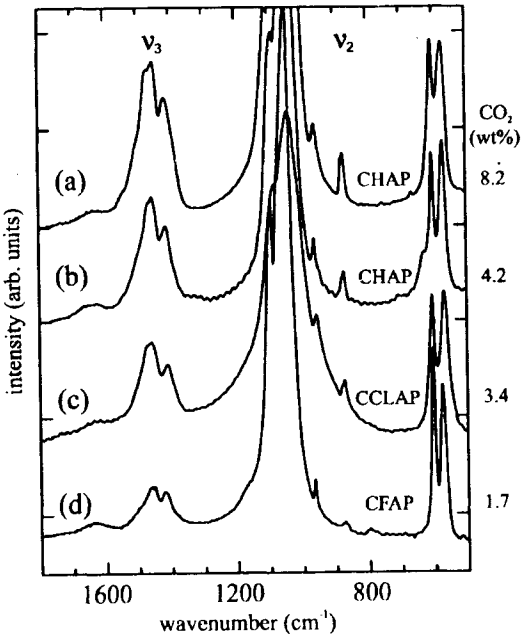

Figure 2. FTIR spectra: (a) CHAP, LM005; (b) CHAP, LM006; (c) CCLAP; (d) CFAP.

Table III. Formula Amounts of Na, A and B Carbonate, X anions and P[a] (*pfu*[b])

Apatite	Expt	Na	A	X	B	P
CHAP[a]	LM005	0.87(3)	1.00(5)	0.0	0.77(3)	5.23
	LM006	0.35(4)	0.52(3)	0.96	0.38(2)	5.62
CFAP	LM130	0.09(3)	0.08(3)	1.84	0.23(1)	5.77
	LM136	0.09(3)	0.16(3)	1.68	0.21(2)	5.79
	LM142	0.11(5)	0.14(3)	1.73	0.23(1)	5.77
CCLAP	LM169	0.40(4)	0.37(3)	1.09	0.57(2)	5.43
	LM171	0.39(3)	0.46(4)	0.97	0.58(3)	5.42
	LM173	0.39(5)	0.42(3)	1.06	0.57(2)	5.44

Notes: [a] Na is based on EPMA; A, B and P on X-ray structure; and X on (2 – 2A) for CHAP and CFAP, and on EPMA for CCLAP
[b] *pfu* is per formula unit

Table IV. Positional and Isotropic Thermal Parameters (Å^2) for CHAP (LM005)

Position	Site Occupancy	*x*	*y*	*z*	*U*
Ca1	0.969(3)	2/3	1/3	0.0014(1)	0.0193(6)
Ca2	0.987(2)	0.9875(1)	0.2499(1)	1/4	0.0181(4)
P	0.871(7)	0.3691(2)	0.3977(2)	1/4	0.0145(7)
O1	0.871(7)	0.4780(3)	0.3232(3)	1/4	0.0151(9)
O2	1.0	0.4644(3)	0.5816(3)	1/4	0.0341(9)
O3	0.903(8)	0.2556(3)	0.3395(3)	0.4263(3)	0.041(1)
C1	0.083	0.046(1)[a]	0.065(1)	0.492(1)	0.025[b]
O5	0.083	0.144(1)	0.220(1)	0.472(1)	0.025
O6	0.083	0.005(1)	0.002(1)	0.662(1)	0.025
O7	0.083	-0.010(1)	-0.028(1)	0.343(1)	0.025
O8	0.064(4)	0.345(3)	0.424(3)	0.448(3)	0.025
O9	0.129(8)	0.512(2)	0.361(2)	1/4	0.025

Notes: [a] *x,y,z* for C1-O7 from rigid body refinement
[b] *U* of C1-O9 not refined

substitution (Table I), but yielded inconclusive results. FTIR spectra of bulk products consistently indicated increased amounts of carbonate in the fine-grained quench apatite but this increase was not reflected in apatite crystallized on a cooling ramp above the solidus. In several experiments on CHAP, excess Na_2CO_3 in the starting mixture resulted in the incorporation of the hydrogen-carbonate (bicarbonate) ion in the *c*-axis structural channel (23). We reported that the hydrogen-carbonate ion is only loosely bound in the apatite channel, and breaks down on aging at room temperature with loss of the volatile decomposition products CO_2 and H_2O. These observations point to a possible role for the apatite channel in mediating acid-base reactions in the body (cf. 25), and help to explain why the channel constituents of the nanoscale crystals of apatite in bone are labile (cf. 8).

X-ray Structures- General Considerations

Results for the X-ray structure refinements of Na-bearing carbonate apatites are summarized in Tables II, III and IV; in the list of structure parameters for CHAP (LM005; Table IV), oxygen atoms O5, O6 and O7 define the type A (channel) carbonate ion and O8 and O9 belong to the type B carbonate ion. Substitution of the carbonate ion into apatite is limited in extent and, unlike atom-for-atom solid solution, introduces new atomic positions. Although the substituents are disordered within the host Ca apatite structure, they are replicated by the hexagonal $P6_3/m$ symmetry and therefore contribute coherent Bragg scattering intensity to the single-crystal diffraction pattern. The diffraction pattern represents only the average structure, a composite of the host structure and the carbonate ions locally ordered in minimum energy locations and configurations. In addition, atoms of the host structure are locally displaced to accommodate the carbonate ions, and this displacement results in anomalous increase in anisotropic displacement parameters (15,22). As a result of these problems, the X-ray structures of carbonate apatites present numerous challenges in interpretation, especially where carbonate contents are very low. In particular, electron densities which may be appreciably less than that of a hydrogen atom and overlap of carbonate and host structure atoms limits the amount of structural information that can be extracted from X-ray structure analysis. It is emphasized that all crystals investigated were of high diffraction quality (e.g. Table II), and the diffraction patterns revealed no evidence of ordering of the carbonate ion defects in the form of superstructure reflections, diffuse scattering or anomalous reflection broadening. However, we argue below that the A and B carbonate ions are present as defect clusters, and these are possibly organized into more extensive domains.

Resolution and refinement of the very weak electron density associated with A and B carbonate atoms in the present Na-bearing carbonate apatite crystals is attributable to the good diffraction quality of the crystals and the high symmetry of the host apatite structures. This statement is supported by the excellent sample-to-sample reproducibility for structure parameters using crystals of different size and shape that excludes significant error from absorption and extinction. Studies on three separate composition series of carbonate apatite crystals grown in the presence of excess sodium carbonate, including CHAP (21), CFAP (24), and carbonate chlorapatite (CCLAP; work in progress), have yielded essentially the same environments for the A and B carbonate ions. These studies encompass a wide range in A and B carbonate contents extending, respectively, from 0.1 and 0.2 per formula unit (*pfu*) in CFAP, to 0.4 and 0.6 *pfu* in CCLAP, and up to 1.0 and 0.8 *pfu* in CHAP (Table III).

Location of type A carbonate

Resolution of the channel (type A) carbonate ion is complicated by overlap of the electron density for the X anion(s), carbon atom and two of the three carbonate oxygens along the c-axis. For partial occupancy of the channel positions, it is not possible to refine independently the occupancy, positional and thermal parameters for these atoms. Fortunately, the channel was wholly occupied by carbonate in one sample of Na-bearing type A-B CHAP (LM005; Tables III, IV; 21), and three-quarters occupied by carbonate in a Na-free type A CHAP (18). The latter apatite had a new space group ($P\bar{3}$), and the carbonate ion was ordered along the apatite channel at $z = 0.5$. This structure established that two of the oxygen atoms lay close to the *c*-axis at about $z = 0.333,0.667$, consistent with a substitution mechanism controlled by charge balance requirements of:

$$[CO_3 = 2(OH)] \quad (1)$$

The plane of the ion was canted about 12° and rotated anticlockwise relative to an ideal model structure. Rigid body refinement, assuming ideal equilateral triangular geometry, then allowed the channel carbonate of a Na-free type A-B CHAP to be refined (20). The plane of this carbonate ion was rotated clockwise in the channel relative to a model channel structure with ideal geometry, and opposite to the rotation for the type A CHAP. Rigid body refinement of the channel carbonate of the Na-bearing type A-B CHAP LM005 resulted in a similar orientation (Fig. 1b). The occupancy of the channel carbonate for the second Na-bearing CHAP in Tables II and III was determined by refining the occupancy of the carbon atom. This carbonate ion configuration was adopted for the Na-bearing CFAP and CCLAP crystals which had a large proportion of X anions, and the carbonate occupancies were determined by refining the occupancy of the third oxygen (O5; Fig. 1b) located off the c-axis close to the channel wall. The electron density for O5 is well resolved even in the CFAP structures which have less than 0.2 carbonate ions per unit-cell. In residual electron density maps at $z = 0.0$ and 0.5, O5 results in well resolved residual peaks in the six equivalent positions consistent with the hexagonal symmetry of the host structure. In Na-free CHAP synthesized at high pressure, there was also evidence of a second location for type A carbonate in a stuffed channel position (19,22). An interesting feature of the CCLAP structures is that the electron density for chlorine is not centered at $z = \pm(0.432,0.068)$, but is spread out along the c-axis. Evidently chlorine is readily displaced by the introduction of the bulky carbonate ion.

Location of type B carbonate

Interpretation of the location of the B carbonate ion is more problematical. Logically, the B carbonate ion is located in the vicinity of the substituted phosphate group and occupies as many of the phosphate oxygen sites as possible. Several studies have noted that the presence of B carbonate is indicated by significant reduction in the occupancy of the P position (12,15,26). Indeed, for the Na-bearing apatites, the phosphorus occupancy decreases systematically with increase in total carbonate content through the series CFAP, CCLAP and CHAP (Tables I, III). Also, our various studies have failed to detect any significant residual electron density in the vicinity of the phosphate group except for that associated with B carbonate lying close to sloping (i.e. inclined to c-axis) faces of the phosphate tetrahedron. In addition, the coupling of A and B carbonate ions discussed below requires the omission of one of the two symmetry-related O3 atoms. In summary, the only likely location for the B carbonate ion in type A-B carbonate apatites is close to the sloping faces (13,19,21). This conclusion is at variance with Rietveld powder neutron diffraction study of francolite from Epirus, Greece, and its heat-treated products (15-17), which suggested that the B carbonate ion was located on the (horizontal) mirror plane, with oxygen atoms at O1, O2 and a third site mid-way between the two symmetry-related O3 sites of the substituted phosphate group. However, this structure assignment was inferred from indirect evidence (e.g. shifts in P-O bond distances and ν_{3c} asymmetric stretching band of phosphate) and lattice dynamics calculations: a third carbonate oxygen was not observed in residual electron density maps.

To complete discussion of the structure refinement procedures, the scattering factors and dispersion corrections for the Ca1 and Ca2 positions were weighted in proportion to the formula amounts of Ca and Na. Average occupancies were refined for CHAP and CCLAP and fixed at 1.0 in CFAP crystals due to their minor content of Na and vacancies. Only two oxygens of type B carbonate were resolved. In CHAP and CCLAP, these were O8, displaced from O3, and O9

displaced from O1, with the third oxygen buried in the electron density of O2. In CFAP, the resolved oxygens were O8, displaced from O2, and O9, displaced from O1. Since these carbonate oxygens were largely overlapped by phosphate oxygens, their occupancies were constrained according to O8 = O9 = (6 – P) in all three composition series. The resulting configuration of the B carbonate in CHAP and CCLAP is shown in Figure 3.

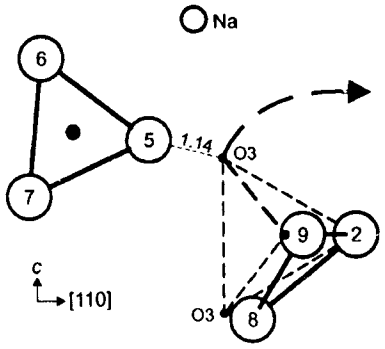

Figure 3. Fragment of structure of Na-CHAP, showing location of type B carbonate ion.

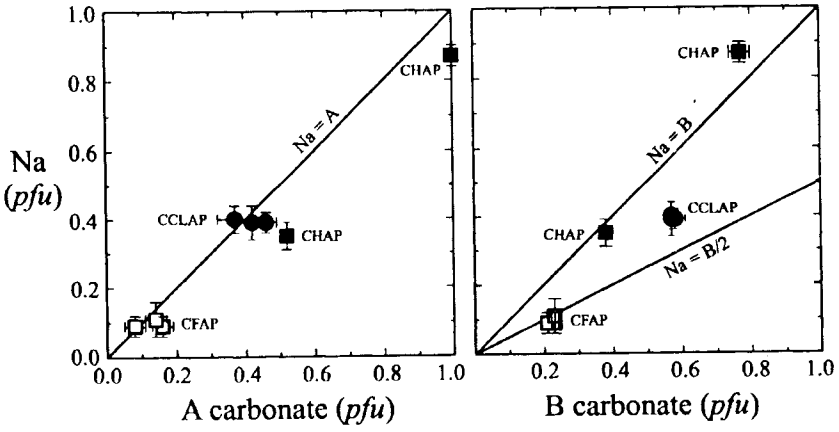

Figure 4. Correlation of Na and A and B carbonate in CHAP, CFAP and CCLAP: *pfu* is per formula unit.

The refined amounts of A and B carbonate in crystals of the three composition series are given in Table III, and correlated in Figure 4. The Na contents in this table were determined independently by electron probe micro-analysis. In Na-bearing CHAP, the formula amounts of Na and A and B carbonate are approximately equal, consistent with the substitution formula

$Ca_{10-y}Na_y[(PO_4)_{6-y}(CO_3)_y][(OH)_{2-2x}(CO_3)_x]$, with $x \approx y \leq 1.0$, and an idealized substitution scheme for B carbonate of:

$$[Na + ({}^{B}CO_3) = Ca + (PO_4)] \quad (2)$$

On the other hand, the CFAP crystals have approximately twice as much B carbonate as A, suggesting a more complex substitution scheme of:

$$[Na + 0.5 \quad + 2({}^{B}CO_3) = 1.5Ca + 2(PO_4)] \quad (3)$$

and giving the substitution formula $Ca_{10-1.5y}Na_{y\ 0.5y}[(PO_4)_{6-2y}(CO_3)_{2y}][F_{2-2x}(CO_3)_x]$, with $x \approx y \approx 0.1$. CCLAP crystals have intermediate proportions of A and B carbonate.

In all cases, the principal charge balancing mechanism in the vicinity of the substituted phosphate group is removal of one of the symmetry-related O3 oxygens. Also, the correlation of Na with B and A carbonate in CHAP and with B/2 and A in CFAP (Fig. 4) confirms that sodium has an active role in the substitution of carbonate into these apatites. Thirdly, in the absence of a proximal B carbonate ion, the off-axis oxygen (O5) of the channel carbonate would be only about 1.1-1.2 Å from an O3 oxygen of the phosphate group (Fig. 3). These three factors strongly suggest that the A and B carbonate ions and Na are locally coupled in the structures of these apatites, to minimize the effects of charge compensation and spatial accommodation. The prohibitively short O5-O3 interaction is eliminated when the O3 oxygen atom in question is removed entirely from the structure and, logically, charge balance requirements favor placing the Na cation closest to this vacant O3 oxygen site.

FTIR Spectroscopy

FTIR spectra of the high-pressure synthesized carbonate apatites are dominated by a complex band at about 1000-1100 cm^{-1} for the asymmetric stretch vibration of the phosphate group, with bands for carbonate at 1400-1600 cm^{-1} (asymmetric stretch vibration; ν_3) and 873-880 cm^{-1} (out-of-plane bend vibration; ν_2) (e.g. Figs. 2, 5). In addition, a weak band for the stretch vibration of structurally-bound OH may be present near 3572 cm^{-1}. Features consistent with the presence of the HPO_4^{2-} ion (27,28) are absent (Fig. 2). Interpretation of the ν_3 carbonate band in the FTIR spectra of apatites with multiple carbonate species is complicated by band overlap and asymmetry of the doublet for the channel (type A) carbonate species (e.g. 22). Band overlap in the 1470-1450 cm^{-1} interval is particularly troublesome. Earlier studies on natural and synthetic Na-free CHAP (e.g. 4,22,29,30) found that type A carbonate was characterized by a doublet band at about 1545 and 1460-1450 cm^{-1} (ν_3) and a singlet band at about 878 cm^{-1} (ν_2), whereas type B carbonate has these bands at about 1450-1455, 1410-1420 and 871 cm^{-1}, respectively. Additional doublet bands at about 1565 and 1505 cm^{-1} in spectra of Na-free A-B CHAP (Fig. 5) were assigned to type A carbonate in a stuffed channel position (22).

However, Fleet and Liu (21) found that in synthetic Na-bearing CHAP the ν_3 doublet for type A carbonate is seemingly shifted to lower wavenumber and into the region normally associated with type B carbonate. A similar shift is present in the spectra of the Na-bearing CFAP and CCLAP crystals, with the CFAP spectra having resolved bands at 1418, 1452 and 1463 cm^{-1} (Fig. 2). Note that the high wavenumber components are weaker in CFAP than for CHAP, consistent with more type B carbonate than type A.

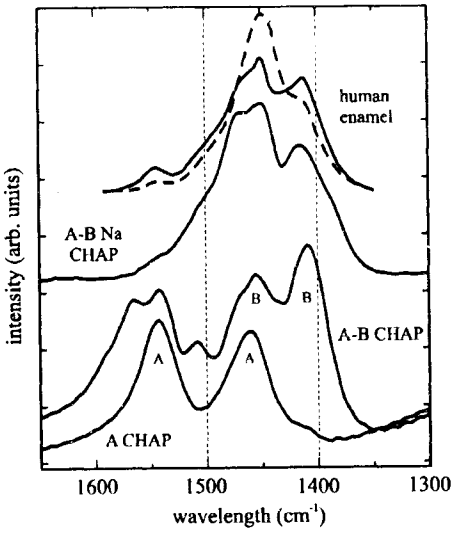

Figure 5. FTIR spectra for human dental enamel, compared with Na-free CHAP and Na-bearing A-B CHAP.

in agreement with the X-ray structure results (Table III). This conclusion is reinforced by the appearance of the compound band for the out-of-plane bend vibration (ν_2), which has a dominant component at 873 cm^{-1} (type B carbonate) and a weak shoulder at 880 cm^{-1} (type A). The separate contributions of type B and A carbonate to the ν_2 bands have been quantified using fitted spectra. The B/A area ratio for CFAP crystals is indeed greater than unity and in good agreement with the corresponding X-ray structure result for all three crystals studied (Table III). In comparison, the B/A ratios in Na-bearing CHAP (LM005) are 0.9 for the ν_2 band areas and 0.8 for the X-ray structure.

A striking feature of the spectra for the three composition series investigated (CHAP, CFAP and CCLAP) is their similarity in the carbonate band regions (Fig. 2). In particular, the composite ν_3 bands have the same overall profile differing only in the amount of carbonate represented and relative proportion of A and B carbonate, with B/A decreasing in the sequence CFAP > CCLAP > CHAP. This spectral feature is consistent with local coupling of the A and B carbonate ions as outlined in the previous section. Furthermore, we suggest that the A and B carbonate ions and Na cation in CHAP are present as a defect cluster within the apatite matrix. It is possible that there exists a degree of intermediate range order, with several A-B pairs organized into columnar *c*-axis domains, analogous to the columnar domains suggested for mixed X anion occupancy in Ca apatites (3,31). As noted above, the X-ray diffraction patterns of these apatites do not reveal any evidence of extensive ordering and it seems unlikely that compositionally distinct domains analogous to those observed in Brazilian gem-grade apatite (32) exist in them.

Apatite Biomineralization

The present synthetic Na-bearing CHAP LM006 has a similar composition to the inorganic fraction of bovine bone and human and pig dental enamel (Table V) and its FTIR spectrum (b in Fig. 2) is similar in the ν_3 region to that of rodent bone mineral (e.g. 9,33) and dental enamel (4,27; present Fig. 5). Therefore, the structure of this type A-B carbonate apatite is probably a good approximation to the overall structure of carbonated hydroxyapatite in bone and enamel. All these materials are Na-bearing carbonate apatites, and their IR spectra are characterized by ν_3 absorption more-or-less confined to the 1400-1500 cm^{-1} spectral interval. An important result of this study is that the proportion of A and B carbonate in the synthetic Na-bearing CHAP has been determined independently by the single-crystal X-ray structure method. It has been independently established that its FTIR spectrum represents approximately equal amounts of A and B carbonate.

Table V. Compositions of Synthetic Na-bearing Carbonate Apatite, Inorganic Fractions of Bone, Tooth Enamel, and Dentine, and Ideal Hydroxyapatite [$Ca_{10}(PO_4)_6(OH)_2$]

	Na-CHAP LM006 (wt%)	Bovine Bone[a] (wt%)	Enamel[a] (wt%)	Dentine[a] (wt%)	Ideal HAP (wt%)
Ca	39.5	36.6	37.6	40.3	39.6
P	17.6	17.1	18.3	18.6	18.5
CO_2	3.5	4.8	3.0	4.8	-
Na	0.81	1.0	0.7	0.1	-
K	-	0.07	0.05	0.07	-
Mg	-	0.6	0.2	1.1	-
Sr	-	0.05	0.03	0.04	-
Cl	-	0.1	0.4	0.27	-
F	-	0.1	0.01	0.07	-
Note: [a] after Ref. 4					

Therefore, the criteria established in the literature for concluding dominance by type B carbonate in biological apatites based on the absence of significant ν_3 absorption intensity beyond 1500 cm^{-1} have to be reconsidered in light of the present study which shows that the ν_3 band intensity for type A carbonate in A-B apatites is sensitively dependent on the composition of the large cation positions, and particularly on the Na content. Type A carbonate is generally assumed to be only a minor component of dental enamel (e.g. 11 to 15%) based on the weak presence of the infrared band near 1545 cm^{-1} (4,27) relative to spectra for Na-free type A and A-B CHAP (e.g. Fig. 5). However, these low estimates for type A carbonate in enamel (and bone) should be revised upward in light of the present study. Biological apatites are not type B carbonate hydroxyapatites. Instead, they appear to be Na-bearing type A-B carbonate hydroxyapatites, the mineral equivalent of LM006, with type A carbonate accounting for up to 50% of total carbonate. The weak and diffuse ν_3 region intensity beyond 1500 cm^{-1} represents either multiple channel sites for carbonate ions (19,22,27), which is not supported by the present X-ray structures, or multiple large-cation (Ca2) configurations around a single carbonate site. It is not possible to deconvolute these spectra without further crystal-chemical insight and in any case the ν_3 region is often of limited utility for study of apatite extracted from bone because it tends to be obscured by absorption bands of functional groups on proteins and glucosaminoglycans (33).

In contrast, the complex ν_2 band appears to better reflect the true proportions of the principal carbonate species. In biological apatites this region is normally deconvoluted to give singlet bands at 878 cm^{-1} (type A carbonate), 871 cm^{-1} (type B carbonate), and 866 cm^{-1} (labile carbonate; e.g. 27,33), although for the present synthetic apatites the first two bands are shifted slightly to 880 cm^{-1} and 873 cm^{-1}, respectively, and a shoulder to the type B carbonate band could represent a minor presence of the labile component. We have noted above that the B/A area ratios from ν_2 region spectra are in good agreement with the X-ray structure site occupancies for the present synthetic CHAP and CFAP crystals. Rey and coworkers report B/A ratios from ν_2 region spectra ranging from 1.1 to 0.8 for pig enamel (27) and 1.4 to 1.2 for various bone samples (cow, human, chicken, rat, and rabbit; 28,33). Clearly, these biological apatites are all type A-B carbonate hydroxyapatites. Finally, we recognize that, although the overall structure of biological apatite appears to have been reproduced, the present synthetic CHAP crystals differ markedly from bone mineral in respect to crystal size, reactivity of the surface layer, and absence of HPO_4^{2-} (e.g. 28,33,34)

CONCLUSIONS

Single-crystal X-ray structures and FTIR spectra for a number of Na-bearing type A-B carbonate hydroxyapatites (CHAP), fluorapatites (CFAP) and chlorapatites (CCLAP) crystallized from carbonate-rich melts at 1000-1350°C and 1.0 GPa indicate local coupling between Na cations and channel (type A) and phosphate (type B) carbonate ions at all carbonate contents investigated. The type B carbonate ion is located close to the sloping faces of the substituted phosphate tetrahedron. Coupling of A and B carbonate ion defects is necessary to avoid the close approach (1.1-1.2 Å) of the off-axis oxygen of the channel carbonate ion to an O3 atom of the phosphate group. These synthetic apatites are appropriate chemical and structural models for biological apatites, which are interpreted as Na-bearing type A-B apatites with channel (type A) carbonate accounting for up to 50% of total carbonate. The X-ray structure site occupancies show that the use of ν_3 region of FTIR spectra to estimate the proportion of type A carbonate in synthetic apatites and biomineralisation is limited by dependence on the composition of the large cation (Ca1,Ca2) positions.

ACKNOWLEDGMENTS

We thank two reviewers for helpful comments and the Natural Sciences and Engineering Research Council of Canada for financial support.

REFERENCES

[1]Y. Pan and M.E. Fleet, Compositions of the apatite-group minerals: Substitution mechanisms and controlling factors, *Rev. Mineral. Geochem.*, **48**, 13-49 (2002).
[2]T.J. White and Z-L. Dong, Structural derivation and crystal chemistry of apatites, Acta Cryst., **B59**, 1-16 (2003).
[3]J.M. Hughes and J. Rakovan, The crystal structure of apatite, $Ca_5(PO_4)_3(F,OH,Cl)$, *Rev. Mineral. Geochem.*, **48**, 1-12 (2002).
[4]J.C. Elliott, Calcium phosphate biominerals, *Rev. Mineral. Geochem.*, **48**, 427-53 (2002).
[5]F. Brudevold, D.E. Gardner, and F.A.Smith, Distribution of fluorine in human enamel, *J. Dental Res.*, **35**, 420-9 (1956).

[6]G.H. McClellan and J.R. Lehr, Crystal chemical investigation of natural apatites, *Am. Mineral.*, **54**, 1374-91 (1969).
[7]B. Wopenka and J.D. Pasteris, A mineralogical perspective on the apatite in bone, *Mater. Sci. Engin.*, C**25**, 131-43 (2005).
[8]G. Cho, Y. Wu, and J.L. Ackerman, Detection of hydroxyl ions in bone mineral by solid state NMR spectroscopy, *Science*, **300**, 1123-7 (2003).
[9]S. Aparicio, S.B. Doty, N.P. Camacho, E.P. Paschalis, L. Spevak, R. Mendelsohn, and A.L. Boskey, Optimal methods for processing mineralized tissues for Fourier transform infrared microspectroscopy, *Calcif. Tissue Int.*, **70**, 422-9 (2002).
[10]Y. Suetsugu, Y. Takahashi, F.P. Okamura, and J. Tanaka, Structure analysis of A-type carbonate apatite by a single-crystal X-ray diffraction method, *J. Solid State Chem.*, **155**, 292-7 (2000).
[11]T.I. Ivanova, O.V. Frank-Kamenetskaya, A.B. Kol'tsov, and V.L. Ugolkov, Crystal structure of calcium-deficient carbonated hydroxyapatite. Thermal decomposition, *J. Solid State Chem.*, **160**, 340-9 (2001).
[12]R.M. Wilson, J.C. Elliott, and S.E.P Dowker, Rietveld refinement of the crystallographic structure of human dental enamel apatites, *Am. Mineral.*, **84**, 1406-14 (1999).
[13]R.M.Wilson, J.C. Elliott, S.E.P. Dowker, and R.I. Smith, Rietveld structure refinement of precipitated carbonate apatite using neutron diffraction data, *Biomaterials*, **25**, 2205-13 (2004).
[14]R.M. Wilson, S.E.P. Dowker, and J.C. Elliott, Rietveld refinements and spectroscopic structural studies of a Na-free carbonate apatite made by hydrolysis of monetite, *Biomaterials*, **27**, 4682-92 (2006).
[15]Th. Leventouri, B.C. Chakoumakos, H.Y. Moghaddam, and V. Perdikatsis, Powder neutron diffraction studies of a carbonate fluorapatite, *J. Mater. Res.*, **15**, 511-7 (2000).
[16]Th. Leventouri, B.C. Chakoumakos, N. Papanearchou, and V. Perdikatsis, (2001) Comparison of crystal structure parameters of natural and synthetic apatites from neutron powder diffraction, *J. Mater. Res.*, **16**, 2600-2606.
[17]A. Antonakos, E. Liarokapis, and Th. Leventouri, Micro-Raman and FTIR studies of synthetic and natural apatites, *Biomaterials*, **28**, 3043-54 (2007).
[18]M.E. Fleet and X. Liu, Carbonate apatite type A synthesized at high pressure: new space group ($P\bar{3}$) and orientation of channel carbonate ion, *J. Solid State Chem.*, **174**, 412-7 (2003).
[19]M.E. Fleet and X. Liu, Location of type B carbonate ion in type A-B carbonate apatite synthesized at high pressure, *J. Solid State Chem.*, **177**, 3174-82 (2004).
[20]M.E. Fleet and X. Liu, Local structure of channel ions in carbonate apatite, *Biomaterials*, **26**, 7548-54 (2005).
[21]M.E. Fleet and Xi Liu, Coupled substitution of type A and B carbonate in sodium-bearing apatite, *Biomaterials*, **28**, 916-26 (2007).
[22]M.E. Fleet, X. Liu, and P.L. King, Accommodation of the carbonate ion in apatite: An FTIR and X-ray structure study of crystals synthesized at 2-4 GPa, Am. Mineral., **89**, 1422-32 (2004).
[23]M.E. Fleet and Xi Liu, Hydrogen carbonate ion in synthetic high-pressure apatite, *Am. Mineral.*, **92**, 1764-7 (2007).
[24]M.E. Fleet and Xi Liu, Accommodation of the carbonate ion in fluorapatite synthesized at high pressure, *Am. Mineral.*, in press (2008).
[25]D.A. Bushinsky, S.B. Smith, K.L. Gavrilov, L.F. Gavrilov, J. Li, and R. Levi-Setti, Acute acidosis-induced alteration in bone bicarbonate and phosphate, *Am. J. Physiol.- Renal Physiol.*, **283**, F1091-7 (2002).

[26]H. Morgan, R.M. Wilson, J.C. Elliott, S.E.P. Dowker, and P. Anderson, Preparation and characterization of monoclinic hydroxyapatite and its precipitated carbonate apatite intermediate, *Biomaterials*, **21**, 617-27 (2000).
[27]C. Rey, V. Renugopalakrishnan, M. Shimizu, B. Collins, and M.J. Glimcher, A resolution-enhanced Fourier transform infrared spectroscopic study of the environment of the CO_3^{2-} ion in the mineral phase of enamel during its formation and maturation. *Calcif. Tissue Int.*, **49**, 259-68 (1991).
[28]H.-M. Kim, C. Rey, and M.J. Glimcher, X-ray diffraction, electron microscopy, and Fourier transform infrared spectroscopy of apatite crystals isolated from chicken and bovine calcified cartilage, *Calcif. Tissue Int.*, **59**, 58-63 (1996).
[29]G. Bonel, Contribution à l'étude de la carbonatation des apatites. I. Synthèse et étude des propriétés physico-chimiques des apatites carbonatées du type A, *Annales de Chimie (Paris, France)*, **7**, 65-88 (1972).
[30]R.Z. LeGeros, O.R. Trautz, E. Klein, and J.P. LeGeros, Two types of carbonate substitution in the apatite structure, *Experimentia*, **25**, 5-7 (1969).
[31]J.C. Elliott, Structure and Chemistry of the Apatites and Other Calcium Orthophosphates, 389 p., Elsevier, Amsterdam (1994).
[32]C. Ferraris, T.J. White, J. Plévert, and R. Wegner, Nanometric modulation in apatite, *Phys. Chem. Mineral.*, **32**, 485-92 (2005).
[33]C. Rey, B. Collins, T. Goehl, I.R. Dickson, and M.J. Glimcher, The carbonate environment in bone mineral: A resolution-enhanced Fourier transform infrared study. *Calcif. Tissue Int.*, **45**, 157-64 (1989).
[34]A.L. Boskey, Mineral analysis provides insights into the mechanism of biomineralization, *Calcif. Tissue Int.*, **72**, 533-6 (2003).